Catalysis Today 169 (2011) 200–206

Contents lists available at ScienceDirect

Catalysis Today

journal homepage: www.elsevier.com/locate/cattod

The mechanism of surface doping in vanadyl pyrophosphate, catalyst for *n*-butane oxidation to maleic anhydride: The role of Au promoter

Silvia Luciani[a,b], Fabrizio Cavani[a,b,*], Vladimiro Dal Santo[c], Nikolaos Dimitratos[d], Michele Rossi[d], Claudia L. Bianchi[e]

[a] *Dipartimento di Chimica Industriale e dei Materiali, ALMA MATER STUDIORUM Università di Bologna, Viale Risorgimento 4, 40136 Bologna, Italy*
[b] *INSTM, Research Unit of Bologna, Italy*
[c] *CNR- Istituto di Scienze e Tecnologie Molecolari, Via C. Golgi 19, 20133 Milano, Italy*
[d] *Dipartimento di Chimica Inorganica Metallorganica e Analitica "L. Malatesta", Università di Milano, Via Venezian 21, 20133 Milano, Italy*
[e] *Dipartimento di Chimica Fisica ed Elettrochimica, Università di Milano, Via Golgi 19, 20133 Milano, Italy*

ARTICLE INFO

Article history:
Received 19 June 2010
Received in revised form 4 December 2010
Accepted 29 December 2010
Available online 11 February 2011

Keywords:
Maleic anhydride
n-Butane
Vanadyl pyrophosphate
Gold
Selectivity
Dopants

ABSTRACT

This paper studies the role of Au as a promoter for vanadyl pyrophosphate, catalyst for *n*-butane oxidation to maleic anhydride. Samples were prepared with a stoichiometric P/V ratio (P/V = 1.0), and then doped with increasing amounts of Au. It was found that the addition of the Au promoter had a profound influence on its catalytic behaviour, as samples containing the greater amount of Au (3 wt%) showed a behaviour that was similar to that of optimal catalysts which were prepared with a slight excess of P. In fact, the presence of Au allowed all the phenomena that typically lead to the worst catalytic behaviour of stoichiometric vanadyl pyrophosphate to be minimised, i.e. both the over-oxidation of vanadium and the development of the very active but poorly selective α_I-$VOPO_4$. This was attributed to the enhanced reducibility of V^{5+} that was observed in Au-doped samples, as compared to the undoped ones.

1. Introduction

The selective oxidation of *n*-butane to maleic anhydride (MA) is catalysed by vanadyl pyrophosphate $(VO)_2P_2O_7$ (VPP), which produces an MA molar yield of between 53 and 65 mol% at *n*-butane conversion of 80–85 mol% [1–3]. While the bulk VPP is always assumed to constitute the core of the active phase, there are different hypotheses regarding the nature of the first atomic layers – i.e. those in direct contact with the gas phase [4–6]. In previous works [7,8], we found that the nature of the surface-active layer is a function of the P/V ratio used for the preparation of the catalyst. A slight excess of P with respect to the stoichiometric requirement for the VPP formation is necessary to aid the formation of the moderately active but selective δ-$VOPO_4$, that is formed during reaction on the surface of VPP. On the contrary, in stoichiometric VPP (P/V atomic ratio 1.0), the formation of highly active but quite unselective α_I-$VOPO_4$ is fostered, especially when the reaction is carried out at temperature intervals of between 340 and 400 °C. The P/V atomic ratio in the most efficient catalysts may range from 1.10 to 1.20.

Another important factor governing the catalytic behaviour of VPP is the presence of promoters. Surprisingly, the numbers of scientific papers devoted to the study of promoters for VPP has been growing in recent years, despite that fact that during the 1980s it seemed that all the possible dopants for this catalyst had been already investigated [9–12]. In fact, a more profound knowledge of the chemical and physical properties of VPP has allowed for a better comprehension of the role of dopants, the promotional effect of which had already been preliminarily evaluated in the past. This is the case of Co and Fe [13–16], Bi [17], Nb [18–20] and alkali metals [21–23]. In his fundamental work aimed at making a rationale on the role of dopants in VPP-based catalysts, Haber and co-workers reported that the doping of VPP with alkaline and alkaline earth metal ions leads to an increase in the effective negative charge on oxygen atoms, which is equivalent to the increase of nucleophilicity of its surface, and accelerates the rate of *n*-butane oxidation to MA [21–23].

In the present work, we report the effect of Au dopant on the catalytic behaviour of VPP. Our aim was to discover how the addition of Au affects both the surface features of VPP and the performance in *n*-butane oxidation.

* Corresponding author at: Dipartimento di Chimica Industriale e dei Materiali, ALMA MATER STUDIORUM Università di Bologna, Viale Risorgimento 4, 40136 Bologna, Italy.
E-mail address: fabrizio.cavani@unibo.it (F. Cavani).

0920-5861/$ – see front matter © 2011 Elsevier B.V. All rights reserved.
doi:10.1016/j.cattod.2010.12.050

2. Experimental

2.1. Preparation of catalysts

The unpromoted and promoted VPO catalysts were prepared according to the following procedure. V_2O_5 (10 g) and H_3PO_4 (85 wt%, 12.9 g), dissolved in an aqueous solution were refluxed for 72 h to form a yellow slurry containing the $VOPO_4{\cdot}2H_2O$ precursor. The water was evaporated and the cake dried for 12 h at 120 °C. Afterwards, the formation of $VOHPO_4{\cdot}0.5H_2O$ (*precursor*) was accomplished by suspending $VOPO_4{\cdot}2H_2O$ in isobutanol and refluxing for 72 h. The whitish-blue slurry was filtered and the resulting paste was dried at 120 °C overnight. The P/V atomic ratio was 1.0. The *precursor* was then thermally treated in reacting atmosphere at 420 °C for a period of 72 h (after this period samples are to be referred to as *fresh* catalysts), and finally resulted in the formation of the desired VPP phase. Catalysts were then used in *n*-butane oxidation for experimental tests in function of temperature; samples finally downloaded from reactor are referred to as *used* catalysts. The 1 wt% Au/VPO and 3 wt% Au/VPO samples were prepared by the pore volume impregnation (incipient wetness) method. The desired amount of $HAuCl_4$ was impregnated onto the *precursor*. The paste was ground and dried at 150 °C overnight and, finally, thermally treated as described above. Samples are denoted with the codes VPO, VPO1Au and VPO3Au, for samples containing 0 (undoped), 1 and 3 wt% Au, respectively.

2.2. Characterisation of catalysts

The characterisation of the catalysts was performed using XRD, BET, XPS, TEM and TPR techniques. X-ray diffraction (XRD) patterns were collected using a Rigaku D III-MAX horizontal-scan powder equipped with a graphite monochromator, operating at 40 kV and 45 mA, and employing nickel-filtered CuKα radiation (λ = 0.1542 nm). The calculation of the crystallite size of the (2 0 0) and (0 2 4) planes is given by the Scherrer equation: $t = 0.9\lambda/(\beta_{hkl} \times \cos\theta_{hkl})$, where t is the crystallite size, λ is the X-ray wavelength of radiation for CuKα, β_{hkl} is the full-width at half maximum (FWHM) at (hkl) peak and θ_{hkl} is the diffraction angle [24].

Single-point BET surface areas of the catalysts were determined using N_2 adsorption at 77 K using a Thermo Quest Surface Area Analyser.

XPS measurements were performed in an M-Probe Instrument (SSI) equipped with a monochromatic Al-Kα source (1486.6 eV) with a spot size of 200 μm × 750 μm and a pass energy of 25 eV, providing a resolution for 0.74 eV. The accuracy of the reported binding energies (BEs) can be estimated to be ±0.2 eV. The quantitative data was checked accurately and reproduced several times (at least 10 times for each sample). Binding energies of C 1s, P 2p, V $2p_{3/2}$ (V^{5+} and V^{4+}), Au 4f and O 1s were determined.

Transmission electron microscopy (TEM) was carried out using a Tecnai F20 transmission electron microscope operating at 200 kV and equipped with a high-angle annular dark field (HAADF) detector for scanning electron microscopy (SEM) and an energy dispersive X-ray (EDX) detector. To obtain suitable samples for TEM characterisation, the catalysts were treated as follows: samples were finely ground and then deposited onto a holey copper carbon grid in the native form. Particle sizes and particle size distributions were determined from the TEM micrographs by measuring the sizes of at least 100 particles. The gold content of the samples was determined by energy dispersive X-ray analysis (EDX).

H_2-TPR measurements were performed using a Micromeritics Pulse Chemisorb 2700 apparatus. An appropriate amount of samples (20 mg ca.) was purged at 100 °C for 2 h in Ar flow (50 mL/min) in a pyrex fixed-bed micro-reactor, and then cooled down. The TPR experiment was conducted on treated sample heating, with rate of 8 °C/min, to 600 °C in a H_2 (5% by vol.)/Ar mixture (1 bar, 50 mL/min).

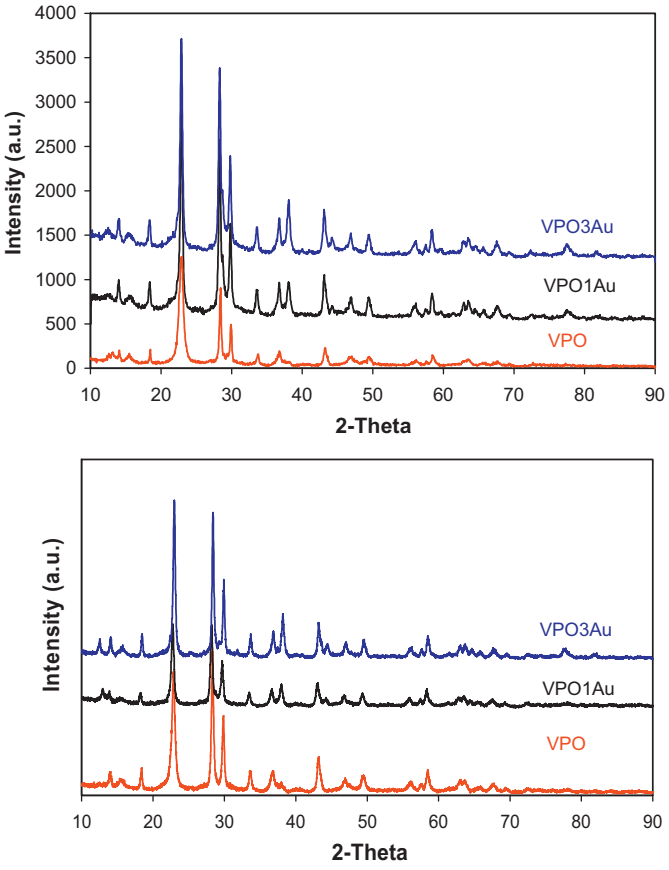

Fig. 1. XRD patterns of fresh samples (top), and of used samples (bottom).

2.3. Catalytic testing

Catalytic tests were carried out in a quartz continuous-flow reactor, loading 0.8 g of catalyst and feeding 1.7% *n*-butane and 17% oxygen (remainder N_2). Overall GHSV was 2160 h^{-1}. Products were analyzed online by sampling a volume of the outlet gas stream and injecting it into a gas chromatograph equipped with an HP-1 column for the separation of C_4 hydrocarbons, formaldehyde, acetic acid, acrylic acid, and MA. A Carbosieve SII column was used for the analysis of oxygen, CO, and CO_2. Fresh catalysts were kept under reacting stream at 400 °C for 20 h before carrying out catalytic experiments; this "equilibration" period is necessary to reach a steady catalytic behaviour.

3. Results and discussion

3.1. Bulk characterisation of catalysts

The characterisation of the VPO, VPO1Au and VPO3Au samples was performed before (with *fresh* samples) and after (with *used* samples) catalytic reaction by XRD. The pattern of fresh VPO indicated the presence of characteristic peaks of well-crystallised $(VO)_2P_2O_7$ phase (JCPDS-01-089-8338) (Fig. 1, top), at $2\theta = 14.1°$, 15.5°, 18.5°, 23.0°, 28.5°, 29.9°, 33.8°, 36.9°, 43.3°, 46.9°, 49.5°, 58.5°, 63.7°, and 67.7°, with three main characteristic peaks at $2\theta = 23.0°$, 28.5° and 29.9°, which correspond to (2 0 0), (0 2 4) and (0 3 2) planes, respectively [25]. The crystallite sizes of the (2 0 0)

Table 1
XRD data for VPO, VPO1Au and VPO3Au catalysts (fresh and used).

Samples	VPP FWHM (2 0 0)	VPP FWHM (0 2 4)	Au FWHM (1 1 1)	VPP[a] t (2 0 0) (nm)	VPP[a] t (0 2 4) (nm)	Au[a] t (1 1 1) (nm)
VPO (fresh)	0.63	0.29	–	13 ± 1	28 ± 2	–
VPO (used)	0.53	0.32		15 ± 1	26 ± 2	
VPO1Au (fresh)	0.41	0.33	0.44	20 ± 2	25 ± 2	19 ± 2
VPO1Au (used)	0.4	0.32	0.41	20 ± 2	25 ± 2	20 ± 2
VPO3Au (fresh)	0.41	0.37	0.42	20 ± 2	22 ± 2	20 ± 2 (16 ± 1)[b]
VPO3Au (used)	0.34	0.26	0.37	24 ± 2	31 ± 2	22 ± 2

[a] Calculation of mean crystallite size based on the Scherrer equation $t = (\kappa \times \lambda)/(\beta_{hkl} \times \cos\theta_{hkl})$.
[b] Mean particle size measured from TEM analysis.

and (0 2 4) planes were calculated as 13 nm and 28 nm, respectively (Table 1).

For VPO1Au, the typical peaks of vanadyl pyrophosphate were also observed, with additional diffraction peaks which are attributable to gold in the metallic state ($2\theta = 38.1^\circ$, 44.2° and 64.6°) (JCPDS-00-002-1095). The calculation of the average gold crystallite size, estimated from the line-width of the Au (1 1 1) diffraction peak at $2\theta = 38.1^\circ$, gave a value of 19 nm. In addition, the crystallite sizes of the (2 0 0) and (0 2 4) VPP planes were 20 nm and 25 nm, respectively. In the case of the XRD pattern of VPO3Au, the average crystallite size of Au was 20 nm, whereas the crystallite sizes of (2 0 0) and (0 2 4) VPP planes were 20 nm and 22 nm, respectively.

These data show that all patterns are characteristic of the VPP phase, and that the addition of Au had only a minor or negligible influence on the FWHM of the (2 0 0) and (0 2 4) VPP planes and on the crystallite sizes in the corresponding planes.

TEM analysis was performed for the fresh VPO3Au, where the size of Au particles was evaluated; Fig. 2 shows HRTEM images of the sample. As can be seen, the presence of Au particles was confirmed while the mean particle size was 16 ± 1 nm. The particle size distribution was rather broad, in the range of 2–69 nm (standard deviation 13). The majority of Au particles were in the range 8–16 nm, whereas a small amount of large gold particles (≥26 nm) were present. The value of mean Au particle size is close to the value obtained from the measurement of the Au crystallite size using the Scherrer equation (20 nm).

The XRD pattern of the used catalysts (Fig. 1, bottom) demonstrated that there was no modification of the structure, thus indicating structural and thermal stability under the studied reaction conditions. The calculation of the crystallite size of (2 0 0) and (0 2 4) VPP planes revealed a small change registered after the catalytic reaction for VPO3Au (Table 1). There was no variation of the crystallite size of Au for both VPO1Au and VPO3Au, thus indicating that under these reaction conditions the growth of Au particle size is not significant.

Table 2
Surface areas of VPO, VPO1Au and VPO3Au catalysts (fresh and used).

Samples	S_{BET} ($m^2\ g^{-1}$) (fresh)	S_{BET} ($m^2\ g^{-1}$) (used)
VPO	14	18
VPO1Au	15	16
VPO3Au	19	21

The surface area analysis was performed on fresh and used samples, as it is shown in Table 2. For fresh VPO, VPO1Au and VPO3Au, the specific surface areas were 14, 15 and 19 $m^2\ g^{-1}$, respectively. As can be observed, no relevant changes in surface area were registered while doping the VPO material with Au. After the catalytic reaction surface areas were 18, 16 and 21 $m^2\ g^{-1}$, respectively.

3.2. XPS analysis

The oxidation state, concentration of surface elements and interaction between Au particles and VPO catalysts were investigated by means of XPS; as an example, Fig. 3 shows the V 2p and O 1s regions for fresh VPO1Au and the Au 4f region for fresh VPO3Au.

The binding energies of V $2p_{3/2}$ peak attributed to V^{4+} and V^{5+} phase are observed typically at 516.9 eV and 518.0 eV, respectively [12,26,27]. Due to the presence of two oxidation states of vanadium, the V $2p_{3/2}$ peak is relatively broad. Therefore, the percentage of surface V^{4+} and V^{5+} has to be calculated using the deconvolution of the V $2p_{3/2}$ peak.

In fresh VPO, two peaks with BE of 517.0 and 518.2 eV are attributed to V^{4+} and V^{5+} oxidation states in agreement with results previously published [24,26–28] (Table 3). The binding energy of P 2p (134 eV) is similar to that of the reported VPP [29–31]. Further-

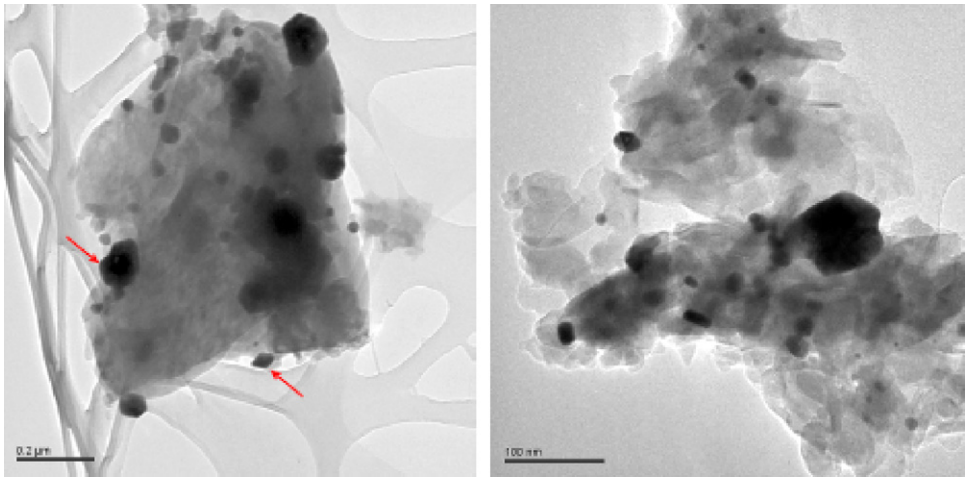

Fig. 2. HRTEM images of fresh VPO3Au; arrows indicate Au particles. Magnification: left Figure 200 nm; right Figure 100 nm.

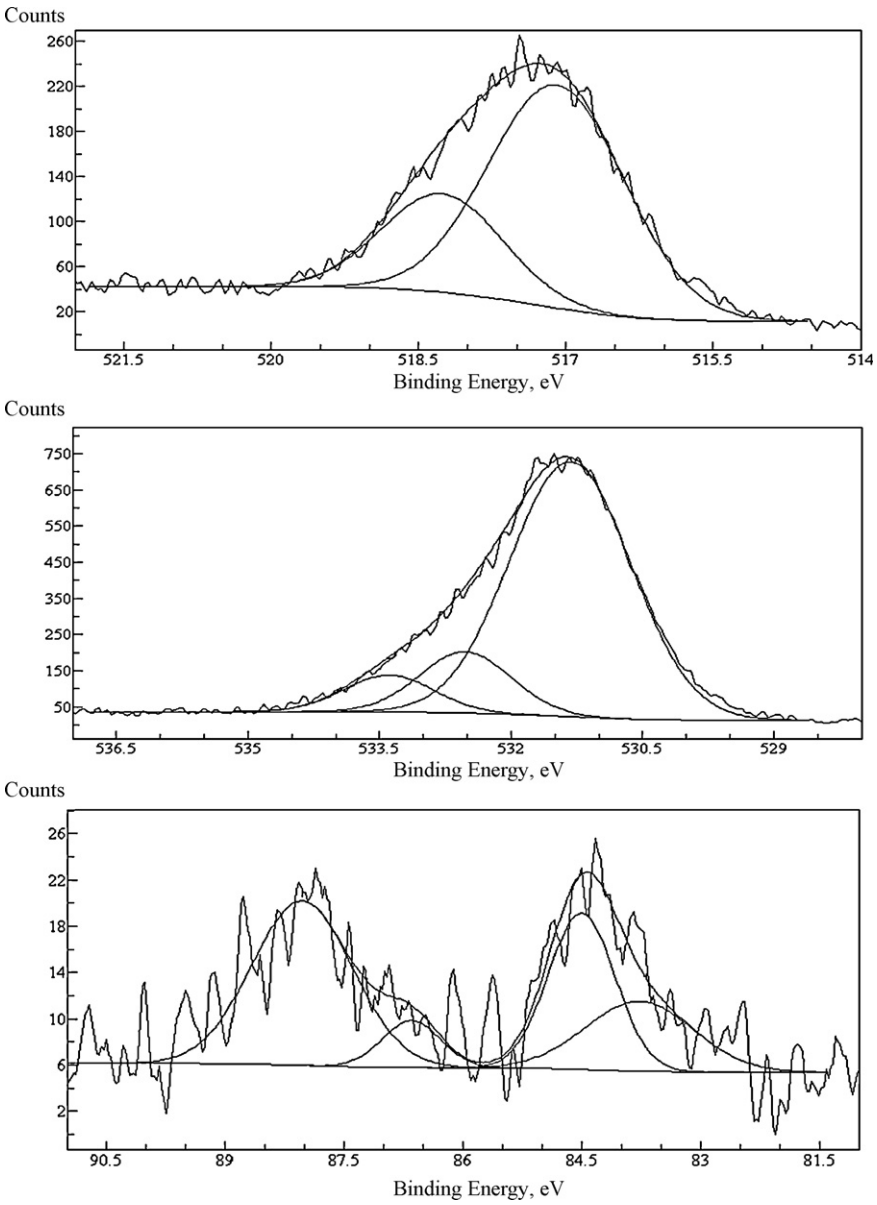

Fig. 3. XPS spectra of the V2p (top), O 1s (center) regions of fresh VPO1Au, and Au 4f region (bottom) of fresh VPO3Au.

more, XPS analysis demonstrated that the P element was enriched on the catalyst surface while the P/V ratio was 2.6 (2.5 for both fresh VPO1Au and VPO3Au): which is in agreement with previous observations [24,26,31,32]. The binding energy of the O 1s level was in the range of 531–533.5 eV. Deconvolution of the O 1s peak revealed the presence of three peaks with binding energies of 531.1 eV, 532.1 eV and 533.0 eV, respectively. The first two peaks correspond to lattice oxygen ions in vanadium phosphates [33], whereas the third peak is related to the presence of surface hydroxide ions and carbonates [34,35].

In the Au 4f region, the presence of Au species is indicated by two peaks, corresponding to Au $4f_{7/2}$ and Au $4f_{5/2}$ transitions; here, values of binding energies will be referred to the Au $4f_{7/2}$ peak. The binding energy at 84.5 eV registered for fresh VPO1Au, suggested the presence of a surface Au species in a positive oxidation state (δ^+). Also for this sample, two V $2p_{3/2}$ peaks with binding energies

Table 3
XPS binding energies of VPO, VPO1Au and VPO3Au catalysts (fresh and used).

Samples	V ($2p_{3/2}$): V^{4+}, V^{5+} BE, eV (%)[a]	Au ($4f_{7/2}$): Au^0, $Au^{\delta+}$ BE, eV (%)[a]	Au/V, atomic ratio
VPO (fresh)	517.0 (84), 518.2 (16)	–	–
VPO (used)	517.3 (58), 518.2 (42)	–	–
VPO1Au (fresh)	517.1 (72), 518.3 (28)	–, 84.5 (100)[a]	0.03
VPO1Au (used)	516.9 (55), 518.3 (45)	Not detectable	–
VPO3Au (fresh)	517.0 (77), 518.2 (23)	83.8 (42)[a], 84.5 (58)[a]	0.03
VPO3Au (used)	517.1 (67), 518.4 (33)	–, 84.8 (100)[a]	0.04

[a] Relative % amount of the different species.

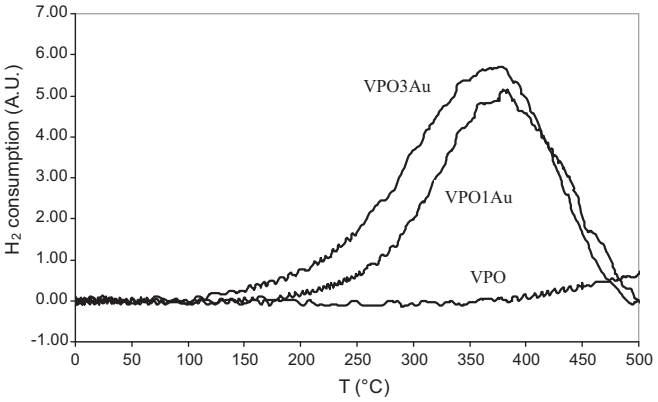

Fig. 4. Temperature-programmed-reduction profiles of fresh catalysts.

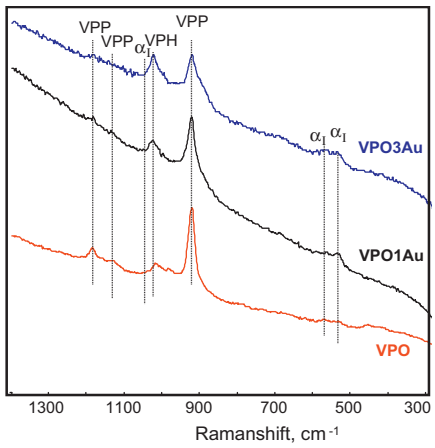

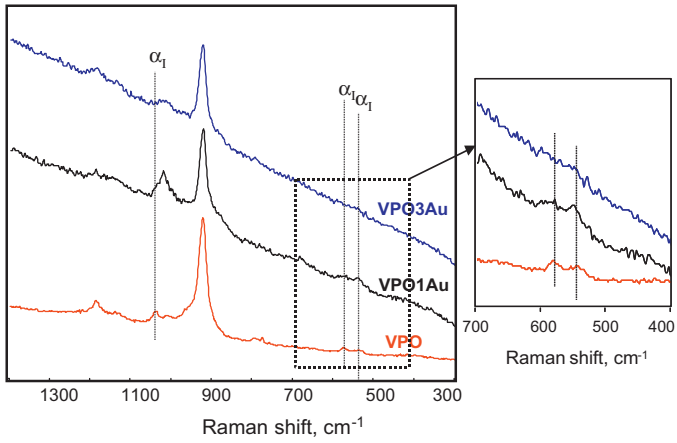

Fig. 5. Raman spectra of fresh (top) and used (bottom) catalysts. VPP, vanadyl pyrophosphate; VPH, $VOPO_4{\cdot}nH_2O$; α_I, α_I-$VOPO_4$.

of 517.1 eV and 518.3 eV are attributed to the V^{4+} and V^{5+} oxidation states.

In the case of fresh VPO3Au, the deconvolution of the Au peak revealed the presence of two oxidation states (83.8 eV and 84.5 eV). The former is attributed to the presence of Au in a metallic state (Au^0) and the latter to Au in a positive oxidation state ($Au^{\delta+}$) [36,37].

After catalytic testing, it was not possible to detect the Au peak for VPO1Au. In the case of VPO3Au, the Au peak, still visible in the used sample, was shifted to a higher value (84.8 eV), thus suggesting the prevailing presence of oxidized Au. The P/V ratio of used catalysts was similar to that of corresponding fresh samples. Regarding the V^{5+}/V^{4+} ratio, it is worth noting that all used samples were more oxidized than the corresponding fresh ones; this is a typical feature of catalysts prepared with the stoichiometric P/V ratio. In fact, during equilibration, VPP catalysts which contain excess P (e.g. with P/V = 1.1) become progressively more reduced, until finally the fraction of V^{5+} detected in used samples is remarkably less than that originally present in fresh catalysts. The opposite phenomenon is observed with samples that do not contain excess P [28]. However, Table 3 shows that the less marked increase of the relative amount of V^{5+} was observed with used VPO3Au, which at the end was the sample containing the lower relative amount of V^{5+}. Thus, it seems that in the presence of a greater amount of Au (i.e. in sample VPO3Au), the latter facilitates the reduction of V^{5+} to V^{4+}, being in turn oxidized to $Au^{\delta+}$.

3.3. TPR analysis

Fig. 4 shows the TPR profile of samples in an H_2/Ar feed. For unpromoted VPO, the reduction process initiated at about 350 °C is followed by a slow increase of the signal up to 500 °C. In Au-doped samples, an intense reduction peak is demonstrated at around 375 °C. The peak onset position depends on the Au loading, and was located respectively at 180 °C for VPO1Au and 120 °C for VPO3Au. The broad peak can be assigned mainly to the reduction of V^{5+} species, however we cannot exclude the contribution of the reduction of $Au^{\delta+}$ species to Au^0, although this contribution will be rather moderate due to the low amount of $Au^{\delta+}$ species. These results are in agreement with recent data, thus demonstrating the easiest reduction of vanadia and molybdena with hydrogen, in the presence of Au particles [38].

3.4. Raman spectroscopy

Fig. 5 compiles Raman spectra of fresh and used catalysts. All samples show main Raman bands attributable to VPP, and additional bands that are attributed to α_I-$VOPO_4$ (1036 cm^{-1}, 540 cm^{-1} and 575 cm^{-1}) [39,40]. The band at Raman shift 1027 cm^{-1} is attributable to a hydrated form of $VOPO_4$ ($VOPO_4{\cdot}nH_2O$). In previous works, we found that the relative amount of VPP and of $VOPO_4$ compounds is affected by the conditions used for thermal treatment and by the P/V ratio used for the preparation of samples; catalysts having a P/V atomic ratio close to the stoichiometric one usually appear to be more oxidized than samples containing excess P [7,8].

Raman spectra of used samples show marked differences; specifically, in the case of VPO1 and VPO1Au, the bands attributable to α_I-$VOPO_4$ are still present, whereas VPO3Au did not show evidence of the presence of this $VOPO_4$ compound. Since XPS demonstrated that even the used VPO3Au was oxidized, although less than used VPO and VPO1Au, this result indicates the possible presence of dispersed V^{5+} sites and not of bulk $VOPO_4$ in VPO3Au, a situation that is conducive to a more selective catalyst [41–43].

At this point, we would like to note the following, as reported in papers previously published [7,8]:

1. The development of α_I-$VOPO_4$ during reaction at temperatures between 340 and 400 °C is a typical feature of samples having P/V ratio of 1.0 [7,8]. α_I-$VOPO_4$ is extremely active but poorly selective to MA. *Ex situ* Raman spectra of used VPO and VPO1Au still show the Raman bands attributable to this compound.
2. In contrast with the behaviour of stoichiometric catalysts, with samples having P/V ratio higher than 1.0 the surface of the catalyst becomes enriched with δ-$VOPO_4$ during reaction [7,8]. This catalyst is moderately active but selective to MA, that explains both why industrial catalysts usually contain an excess of P and why often P-containing organic compounds (gas-phase promot-

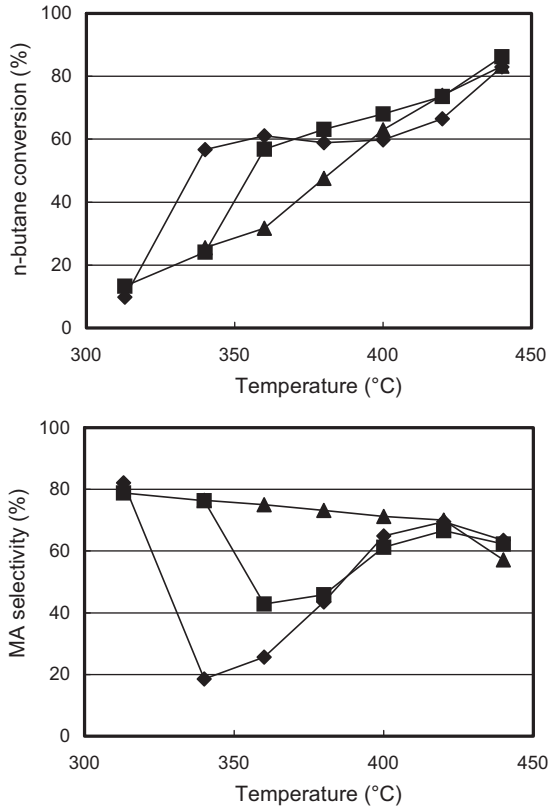

Fig. 6. Conversion of *n*-butane (top) and selectivity to MA (bottom) in function of the reaction temperature. "Equilibrated" catalysts: VPO (♦), VPO1Au (■) and VPO3Au (▲).

ers) are fed to the reactor in the aim of keeping high selectivity to MA during operation. *Ex situ* Raman spectra of these samples may still clearly show band attributable to δ-$VOPO_4$, or even be almost completely reduced (with only trace amount of V^{5+}), in function of the procedure adopted for catalyst downloading from the reactor [8].

In the case of our used samples, the main point concerns the presence of α_I-$VOPO_4$ in VPO and VPO1Au, but not in VPO3Au; this observation was somewhat unexpected, since all samples were prepared with stoichiometric P/V ratio, that according to previous results should cause the formation of the unselective α_I-$VOPO_4$. This means that in VPO3Au, the amount of Au dopant not only allows the formation of V^{5+} that develops on VPO surface during reaction (as inferred from XPS characterisation of used catalysts) to be limited, but also hinders the formation of bulk, unselective $VOPO_4$ compounds.

Based on the characterisation of used catalysts, we would expect similar catalytic behaviour for VPO and VPO1Au samples – as typically observed with VPP prepared with a stoichiometric P/V ratio – and different behaviour for VPO3Au. In this latter case, the characteristics of the used sample are those typically observed with VPP samples containing excess P. Reactivity experiments will confirm this expectation.

3.5. Reactivity tests

Fig. 6 reports the effect of temperature on *n*-butane conversion and on selectivity to MA for equilibrated samples. It is shown that VPO3Au demonstrated both the expected increase in *n*-butane conversion when the reaction temperature was raised, and a slight decline of selectivity to MA. Conversely, both VPO and, to a minor extent, VPO1Au, demonstrated anomalous behaviour; in fact, with VPO the conversion rapidly increased in the 310–350 °C temperature range, then remained more or less constant up to 400 °C, when it finally increased again. Correspondingly, the selectivity to MA demonstrated a dramatic fall at above 300 °C, reaching a minimum value at 340 °C, and then increased again; the maximum value being obtained at 420 °C. The following observations are especially noteworthy:

1. This behaviour was fully reproduced when the reaction temperature was increased and then decreased several times; in other words, the observed phenomena were not due to some effects attributable to irreversible changes in catalyst characteristics.
2. The three samples performed similarly in the temperature range of 400–440 °C, but they performed quite differently in the intermediate temperature range of 340–400 °C.
3. The fall of selectivity to MA shown by VPO and VPO1Au at above 300–320 °C was not simply due to the anomalous rise of conversion. In fact, it must be noted that the selectivity to MA became too low to be attributed solely to the enhanced contribution of consecutive combustions.

The behaviour shown by VPO was that typically observed with VPP-based catalysts having a stoichiometric P/V ratio; it was attributed to the development of the unselective α_I-$VOPO_4$ compound in the intermediate temperature range [7,8], as is also confirmed by Raman spectra of our used VPO sample (Fig. 5). Stoichiometric VPP, however, developed the selective and moderately active δ-$VOPO_4$ phase at above 400 °C, which explains why the VPO sample demonstrated good catalytic behaviour at high temperatures. The same behaviour should have also been expected for VPO1Au and VPO3Au, since both doped samples were prepared with stoichiometric P/V = 1.0 ratio. Conversely, VPO3Au demonstrated the typical behaviour of VPP catalysts containing excess P, that contrasts with the P/V ratio used for its preparation, but fully agrees with the characterisation of the used sample. Finally, VPO1Au demonstrated a catalytic behaviour that is intermediate between those of VPO and VPO3Au.

In TiO_2–Au catalysts for propene oxidation with H_2/O_2, a particular feature is the presence of a chemical interaction between titanium and gold, which confers to the system the ability to generate the active species for olefin epoxidation [44]. For this reason, one major parameter affecting activity is gold dispersion, and hence the contact area between the two components. It was proposed that the active Ti-hydroperoxo species is formed by adsorption of O_2 onto Au, with the development of an Au^+–O_2^- species, which then reacts with H_2 to generate hydrogen peroxide [45]. In our case, even though a possible role of a Au^+–O_2^- species in MA formation cannot be ruled out, the relatively large crystallite size of Au, which is similar to that of the VPP (Table 1), suggests that Au is not highly dispersed over the VPP surface.

With our samples, all the results obtained are conducive to the conclusion that Au plays the same role as that of having excess P in VPP catalysts. $Au^{\delta+}$ species are likely present on the surface of Au metal particles in calcined fresh VPO1Au and VPO3Au, but we cannot exclude that indeed oxidized Au species are highly dispersed on the surface of VPP, in chemical interaction with V sites. During the catalytic reaction, the relative amount of the oxidized Au increases, becoming the only detectable Au species by means of XPS in VPO3Au. Therefore, Au helps in keeping a lower average oxidation state for surface V, and in developing an optimal amount of V^{5+} on the VPP surface and limiting the formation of the very active but unselective bulk α_I-$VOPO_4$. This effect is proportional to the Au amount loaded; a relatively small amount of Au provides a limited improvement of performance as compared to the undoped catalyst, whereas a loading as high as the 3 wt% Au finally allows

the optimal catalytic performance to be obtained. This may also offer the advantage that the co-feeding of P-containing compounds during industrial operation may no longer be required to maintain a P-enriched catalytic surface. A similar effect was reported by Andreeva et al. [46], for the Au–V_2O_5/TiO_2 system, in which the temperature for V^{5+} reduction was considerably lowered with respect to the corresponding unpromoted system; this effect was attributed to a weakening of both V=O and V–O–Ti bonds, in chemical interaction with Au.

4. Conclusions

The doping of vanadyl pyrophosphate with Au in catalysts prepared with a stoichiometric P/V ratio (P/V = 1.0) allowed considerably improving the catalytic performance as compared to the undoped samples. In fact, the behaviour of the VPP doped with 3 wt% Au was as good as that one typically shown by VPP catalysts prepared with an excess P. The higher the amount of Au loading, the greater the improvement of catalytic behaviour as compared to that of the undoped sample. It was found that Au limits the over-oxidation of catalyst surface that is typically observed with stoichiometric VPP, and also hinders the development of bulk unselective $VOPO_4$ compounds.

References

[1] N. Ballarini, F. Cavani, C. Cortelli, S. Ligi, F. Pierelli, F. Trifirò, C. Fumagalli, G. Mazzoni, T. Monti, Top. Catal. 38 (2006) 147.
[2] J.C. Volta, C.R. Acad. Sci. Paris IIc Chim. 3 (2000) 717.
[3] E. Bordes, Top. Catal. 15 (2001) 131.
[4] H. Berndt, K. Buker, A. Martin, A. Brückner, B. Lücke, J. Chem. Soc. Faraday Trans. 91 (1995) 725.
[5] V.V. Guliants, J.B. Benziger, S. Sundaresan, N. Yao, I.E. Wachs, Catal. Lett. 32 (1995) 379.
[6] E. Bordes, Catal. Today 16 (1993) 27.
[7] F. Cavani, S. Luciani, E. Degli Esposti, C. Cortelli, R. Lenza, Chem. Eur. J. 16 (2010) 1646.
[8] F. Cavani, D. De Santi, S. Luciani, A. Löfberg, E. Bordes-Richard, C. Cortelli, R. Leanza, Appl. Catal. A 376 (2010) 66.
[9] G.J. Hutchings, Appl. Catal. 72 (1991) 1.
[10] F. Cavani, F. Trifirò, Catalysis 11 (1994) 246.
[11] B.K. Hodnett, Catal. Rev. Sci. Eng. 27 (1985) 373.
[12] G.J. Hutchings, R. Higgins, J. Catal. 162 (1996) 153.
[13] F. Cavani, A. Colombo, F. Trifirò, M.T. Sananes Schulz, J.C. Volta, G.J. Hutchings, Catal. Lett. 43 (1997) 241–247.
[14] C. Carrara, S. Irusta, E. Lombardo, L. Cornaglia, Appl. Catal. A 217 (2001) 275.
[15] S. Sajip, J.K. Bartley, A. Burrows, C. Rhodes, J.C. Volta, C.J. Kiely, G.J. Hutchings, Phys. Chem. Chem. Phys. 3 (2001) 2143.
[16] L. Cornaglia, S. Irusta, E.A. Lombardo, M.C. Durupty, J.C. Volta, Catal. Today 78 (2003) 291.
[17] Y.H. Taufiq-Yap, K.P. Tan, K.C. Waugh, M.Z. Hussein, I. Ramli, M.B. Abdul Rahman, Catal. Lett. 89 (2003) 87.
[18] I. Matsuura, T. Ishimura, S. Hayakawa, N. Kimura, Catal. Today 28 (1996) 133.
[19] A.M. Duarte de Farias, W. De, A. Gonzalez, P.G. Pris de Oliveira, J.G. Eon, J.M. Herrmann, M. Aouine, S. Loridant, J.C. Volta, J. Catal. 208 (2002) 238.
[20] F. Cavani, F. Pierelli, F. Ghelfi, G. Mazzone, C. Fumagalli, Eur. Patent 1,514,598 A1 (2005), assigned to Lonza.
[21] J. Haber, Catal. Today 142 (2009) 100.
[22] V.A. Zazhigalov, J. Haber, J. Stoch, I.V. Bacherikova, G.A. Komashko, A.I. Pyatnitskaya, Appl. Catal. A 134 (1996) 225.
[23] V.A. Zazhigalov, J. Haber, J. Stoch, I.V. Bogatskaya, I.V. Bacherikova, Stud. Surf. Sci. Catal. B 101 (1996) 1038.
[24] P.H. Klug, E. Alexander, X-ray Diffraction Procedures for Polycrystalline and Amorphous Materials, 2nd ed., John Wiley and Sons, 1974.
[25] A.M.D. de Farias, W.D. Gonzalez, P.G.P. de Oliveira, J.G. Eon, J.M. Herrmann, M. Aourine, S. Loridant, J.C. Volta, J. Catal. 208 (2002) 238.
[26] M. Abon, K.E. Bere, A. Tuel, P. Delichere, J. Catal. 156 (1995) 28.
[27] M.T. Sananes-Schulz, F. Ben Abdelouahab, G.J. Hutchings, J.C. Volta, J. Catal. 163 (1996) 346.
[28] S. Albonetti, F. Cavani, F. Trifiro, P. Venturoli, G. Calestani, M. Lopez Granados, J.L.G. Fierro, J. Catal. 160 (1996) 52.
[29] X. Wang, L. Xu, X. Chen, W. Ji, Q. Yan, Y. Chen, J. Mol. Catal. A 206 (2003) 261.
[30] J. Haber, V.A. Zazhigalov, J. Stoch, L.V. Bogutskaya, I.V. Batcherikova, Catal. Today 33 (1997) 39.
[31] S. Irusta, A. Boix, B. Pierini, C. Caspani, J. Petunchi, J. Catal. 187 (1999) 298.
[32] L.M. Cornaglia, E.A. Lombardo, Appl. Catal. A 127 (1995) 125.
[33] B. Solsona, V.A. Zazhigalov, J.M. Lopez Nieto, I.V. Bacherikova, E.A. Diyuk, Appl. Catal. A 249 (2003) 81.
[34] J. Stoch, J. Gablankowska-Kukucz, Surf. Interface Anal. 17 (1991) 165.
[35] F. Richter, H. Papp, G.U. Wolf, Th. Götze, B. Kubias, Fresenius J. Anal. Chem. 365 (1999) 150.
[36] A.M. Visco, F. Neri, G. Neri, A. Donato, C. Milone, S. Galvagno, Phys. Chem. Chem. Phys. 1 (1999) 2869.
[37] F.W. Chang, H.Y. Yu, L.S. Roselin, H.C. Yang, Appl. Catal. A 290 (2005) 138.
[38] M. Ruszel, B. Grzybowska, M. Gasior, K. Samson, I. Gressel, J. Stoch, Catal. Today 99 (2005) 151.
[39] F. Ben Abdelouahab, R. Olier, N. Guilhaume, F. Lefebvre, J.C. Volta, J. Catal. 134 (1992) 151.
[40] F. Ben Abdelouahab, J.C. Volta, R. Olier, J. Catal. 148 (1994) 334.
[41] G.J. Hutchings, A. Desmartin-Chomel, R. Olier, J.C. Volta, Nature 368 (1994) 41.
[42] K. Ait-Lachgar, M. Abon, J.C. Volta, J. Catal. 171 (1997) 383.
[43] K. Ait-Lachgar, A. Tuel, M. Brun, J.M. Herrmann, J.M. Krafft, J.R. Martin, J.C. Volta, J. Catal. 177 (1998) 224.
[44] T. Hayashi, K. Tanaka, M. Haruta, J. Catal. 178 (1998) 566.
[45] J.J. Bravo-Suarez, K.K. Bando, J. Lu, M. Haruta, T. Fujitani, S.T. Oyama, J. Phys. Chem. C 112 (2008) 1115.
[46] D. Andreeva, T. Tabakova, L. Ilieva, A. Naydenov, D. Mehanjiev, M.V. Abrashev, Appl. Catal. A 209 (2001) 291.